

A Long π -Conjugated Poly-*para*-Phenylene-Based Polymeric Segment of Single-Walled Carbon Nanotubes

Qiang Huang, Mengmeng Zhang, Jinyi Wang, Shengda Wang, Yayu Wu, Shangfeng Yang, Pingwu Du*

Hefei National Laboratory for Physical Sciences at Microscale, Key Laboratory of Materials for Energy Conversion, Chinese Academy of Sciences, Department of Materials Science and Engineering, *iChEM*, University of Science and Technology of China (USTC), 96 Jinzhai Road, Hefei, Anhui Province, 230026, P. R. China.

Supporting Information Placeholder

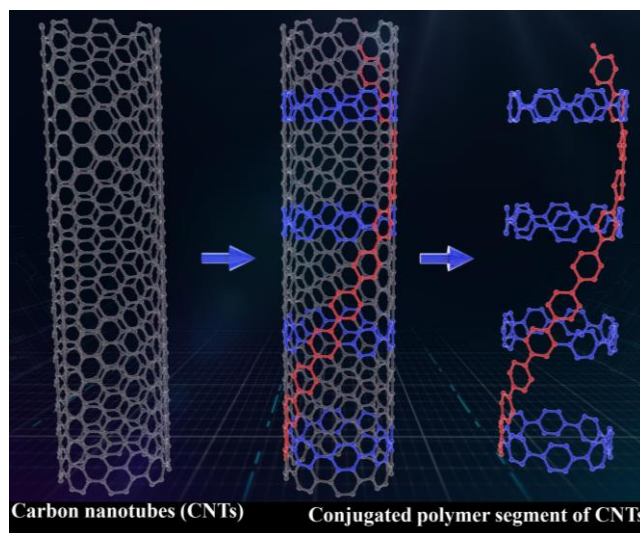
ABSTRACT: Conjugated polymers have attracted much attention for many years and have applications in various organic devices. Carbon nanotubes can be considered as all-carbon tube-shaped conjugated polymers containing only sp^2 -bonded atoms, which play an important role in nanotechnology and nanoelectronics. So far, no study has reported the realization of long π -conjugated polymers as diameter-specified carbon nanotube segments. Herein, we report the first synthesis of a π -conjugated polymeric segment (**PS1**) of armchair single-walled carbon nanotubes. **PS1** is achieved by a rationally designed synthesis of a bifunctionalized cyclo-*para*-phenylene monomer, followed by inserting these ring-shaped units into the conjugated poly-*para*-phenylene backbone. Our **PS1** was fully characterized by gel permeation chromatography (GPC) combined with NMR, FTIR, and Raman spectra. Its photophysical and unique electronic properties were also investigated. Possessing unique structural and physical properties, this long π -extended polymer **PS1** can provide new insight for the development of bottom-up syntheses of uniform carbon nanotube segments and potential applications in electron-transport devices.

As a well-known prototype conjugated polymer, poly-*para*-phenylene (PPP) polymers have been widely studied, resulting in various synthesis approaches¹⁻³ and the fabrication of photoactive devices.⁴⁻⁷ However, almost all direct aryl-aryl coupling reactions from 1,4-dihalobenzenes in solution to produce unsubstituted PPP lead to only low molecular weight oligomers (< 8 units).³ PPP is an insulator in neutral form, but its conductivity can increase to >100 S·cm⁻¹ after chemical doping.⁸⁻⁹ From the point of view of chemical synthesis, PPP contains only sp^2 -carbon atoms and can be considered as conjugated segments of many carbon allotropes such as graphene, graphene nanoribbons, and carbon nanotubes (CNTs). Recently, Basagni and coworkers used a stepwise on-surface polymerization reaction to synthesize oriented graphene nanoribbons *via* the key intermediate of a PPP polymer.¹⁰ On the other hand, PPP polymers can also form carbon nanotube structures if these PPP polymers can be connected into cyclic conjugated structures with a fixed orientation.

Although CNTs have attracted much attention due to their unique electronic, optical, thermal, mechanical, and chemical properties,¹¹⁻¹³ the practical applications of CNTs are significantly limited. Several major problems still exist, such as having no reliable methods to control the alignment during nanotube growth, difficulty in growing nanotubes with a fixed diameter and chirality, and no efficient method to separate random nanotube mixtures.¹⁴⁻¹⁵ Hence, the chemical synthesis of structurally uniform CNTs and highly conjugated CNT segments, is still a great challenge in chemistry and material science. In the last few years, bottom-up synthesis has emerged as a promising strategy and attracted much attention in the quest to develop different curved *and/or* cyclic aromatic structures.¹⁶⁻³³ However, almost all the reported small precursors

are CNT segments possessing only very limited 1D π -conjugated systems at the molecular scale.

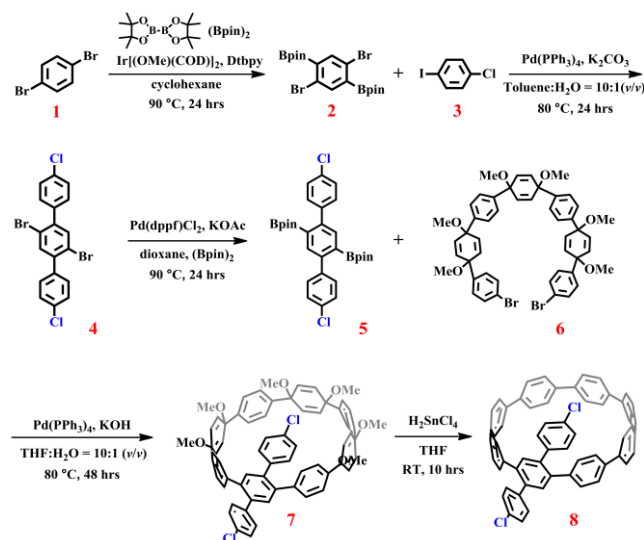
To obtain a real CNT, it is highly desirable to extend the π systems longitudinally. Scott and coworkers proposed a Diels-Alder cycloaddition/rearomatization strategy to grow uniform diameter, single-chirality carbon nanotubes from molecular hydrocarbon templates³⁴ and this strategy has been successful for π -extension of small polyaromatic hydrocarbons. In 2014, using a surface-catalyzed cyclodehydrogenation reaction, Fasel and coworkers obtained ultrashort singly capped [6,6]armchair nanotube seeds on a Pt(111) surface based on a hemispherical end-cap molecular template.³⁵ Later, Zhu and coworkers successfully achieved nearly pure single-walled carbon nanotube (SWCNT) semiconductors based on structurally well-defined molecular end-caps to initiate nanotube growth.³⁶



Scheme 1. The design of a long π -extended poly-*para*-phenylene-based polymeric segment of armchair [8,8]single-walled carbon nanotube.

Herein we report the synthesis of a novel π -extended polymer (**PS1**) containing a cyclic conjugated macrocycle and a PPP backbone, which is a polymer constructed entirely from sp^2 -hybridized carbon atoms and represents the first polymeric segment of armchair [8,8]SWCNT. Possessing both linear and cyclic π -extended system, this conjugated polymer segment closely resembles a CNT. In this study, we design a bifunctionalized cyclo-*para*-phenylene that mimics the curved cyclic polyphenylene part of a CNT and a

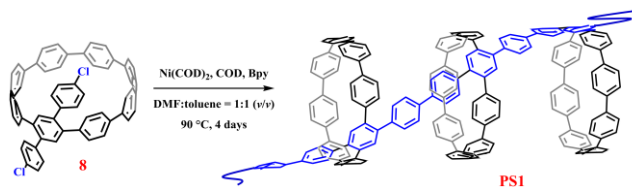
linear PPP backbone that mimics the linear polyphenylene part along the 1D direction of the CNT, as shown in Scheme 1. Our **PS1** was fully characterized by gel permeation chromatography (GPC), as well as ^1H NMR, Fourier transform infrared (FTIR), and Raman spectroscopies. In addition, its photophysical and electronic properties were investigated by UV-vis spectroscopy, fluorescence spectroscopy, time-resolved fluorescence decay, and the space charge limited current methods.



Scheme 2. Synthesis procedure for the pinacol boronic ester **5** and bifunctionalized macrocyclic nanoring monomer **8**.

The challenge of achieving the designed **PS1** is to synthesize bifunctionalized cyclo-*para*-phenylene precursors with suitable bi-functional groups for polymerization. Our synthesis strategy is to connect the curved component and the bifunctionalized component into a cyclic molecule by a Pd-catalyzed Suzuki coupling reaction. The synthesis procedure of the bifunctionalized component is summarized in Scheme 2. Initially, 1,4-dibromo-2,5-phenylenediboronate (**2**) was synthesized from 1,4-dibromobenzene (**1**) by an iridium-catalyzed borylation reaction. Then, Suzuki-Miyaura coupling between **2** and 1-chloro-4-iodobenzene (**3**) in the presence of $[\text{Pd}(\text{PPh}_3)_4]$ catalyst produced compound **4** with a yield of >60%. Next, the Miyaura borylation reaction between compounds **4** and bis(pinacolato)diboron was conducted in dioxane at 90 °C to produce the bifunctionalized component precursor **5** with a good yield of >85%.

With the bifunctionalized component **5** in hand, the subsequent synthesis is embeds **5** into the ring-shaped carbon macrocyclic structure to fabricate the molecular bifunctionalized precursor **7** (Scheme 2). Under the standard conditions of the Pd-catalyzed Suzuki-Miyaura coupling reaction, the bifunctionalized component **5** reacted with a curved precursor **6**²⁸ to give the key macrocycle intermediate **7**. The targeted macrocyclic monomer **8** was then successfully obtained as a yellow solid after a reductive aromatization reaction with H_2SnCl_4 . All these small molecules were fully characterized by ^1H NMR, ^{13}C NMR, and mass spectrometry (Figures S1-S8). In the last step, a polymerization reaction using **8** was carried out in dry DMF/toluene (v/v, 1:1) by nickel-mediated Yamamoto homocoupling reaction (Scheme 3). Finally, the π -extended polymer **PS1** was obtained as a yellow solid with an excellent yield of >75%.



Scheme 3. Synthesis of the conjugated PPP-based polymer **PS1**.

The successful synthesis of polymer **PS1** from monomer **8** was confirmed by the combination of GPC, ^1H NMR, FTIR, and Raman spectroscopies. The weight-average molecular weight (M_w), relative number-average molecular weight (M_n), and weight distribution of **PS1** were measured by GPC (Figure 1a). The molecular weight distribution of **PS1** shows a single broad peak with a polydispersity index of 1.44 and the number-averaged molecular weight is 16900 using polystyrene is used as the standard. To fully assign the aromatic protons in **8**, we recorded the 2D ^1H - ^1H COSY NMR spectrum (Figure S9). The multiplet at 7.53-7.48 ppm is correlated with the proton signal at 7.33 ppm, suggesting that the signal at 7.53-7.48 can be assigned to the **d** site and the doublet at 7.33 ppm belongs to the **c** site. Moreover, this proton signal at 7.24-7.18 ppm is correlated with the proton signal at 7.05-6.99 ppm, confirming the latter can be ascribed to the **a** site. It is found that, in **PS1**, **d** site and **c** site contain most of the protons (Figure 1b) and there are almost no protons at **a** site in **8**. This result indicates that polymer **PS1** has been successfully formed without destroying the cyclic structure of the monomer **8** unit.

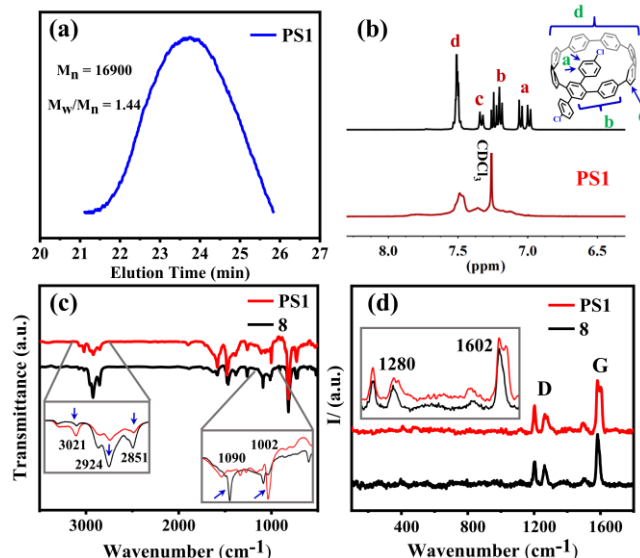


Figure 1. (a) GPC trace of **PS1**. (b) ^1H NMR spectra of **PS1** (red) and **8** (black) in CDCl_3 . (c) FTIR spectra of **PS1** (red) and monomer **8** (black). (d) Raman spectra (excited at 633 nm) of **PS1** (red) and **8** (black).

The FTIR spectra of **PS1** and **8** are shown in Figure 1c. The peak at $\sim 810\text{ cm}^{-1}$ in the spectra of both **PS1** and **8** is a characteristic of out-of-plane C-H deformation from a *para*-disubstituted benzene ring vibration. The absorbance above 3000 cm^{-1} (at 3021 cm^{-1} for **PS1**) can be assigned to the aromatic C-H stretching vibrations of benzene rings. The C-H stretching peaks at 2924 cm^{-1} and 2851 cm^{-1} are broad in monomer **8**, and the intensities of these peaks strongly decrease for **PS1**. In addition, **8** shows an intense peak at 1090 cm^{-1} which completely disappears in the spectrum of **PS1**. In sharp contrast, a new peak is generated for **PS1** at 1002 cm^{-1} and a

similar peak was also observed in the FTIR spectrum of PPP polymers.³⁷ These FTIR results demonstrate that monomer **8** has been transformed into polymer **PS1**.

Moreover, Figure 1d shows the Raman spectra of **PS1** (red plot) and **8** (black plot). In previous studies, the Raman peaks of PPP were located at 1215, 1285 and 1602 cm^{-1} ³⁷ and the peaks of [8]cyclo-*para*-phenylene at 1200, 1262, 1505, and 1582 cm^{-1} .³⁸ For **8**, the main peaks are the D-band (1202 cm^{-1} and 1262 cm^{-1}) associated with carbon macrocycle breathing, the G-band (1582 cm^{-1}) associated with C-C stretching, and a small peak at 1503 cm^{-1} which is a peak associated with the G-band. For **PS1**, the main peaks of the Raman spectrum are located at 1202, 1264, 1280, 1505, 1582, and 1602 cm^{-1} . Four of these peaks in **PS1** (1202, 1264, 1505 and 1582 cm^{-1}) are consistent with the peaks for **8**. Interestingly, compared to the Raman peaks in PPP, the other two peaks in **PS1**, located at 1280 and 1602 cm^{-1} , are comparable to the signals in PPP at 1215, 1285, and 1602 cm^{-1} , indicating the presence of the one-dimensional PPP backbone. The Raman spectra of **PS1** and **8** further provide clear evidence of the presence of both cyclo-*para*-phenylene and linear PPP structures.

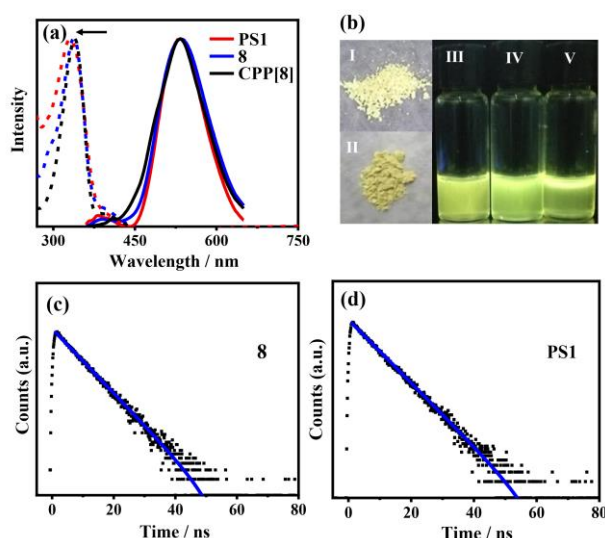


Figure 2. (a) UV-vis absorption (dashed dot) and fluorescence (solid) spectra of **PS1** (red), monomer **8** (blue), and **CPP[8]** ([8]cyclo-*para*-phenylene, black) in CH_2Cl_2 . (b) (I) Solid powder of monomer **8**; (II) Solid powder of **PS1**; **PS1** (III), **8** (IV), and **CPP[8]** (V) in CH_2Cl_2 solution under UV irradiation at $\lambda = 365$ nm. Emission lifetimes for **8** (c), **PS1** (d) in CH_2Cl_2 .

The **PS1** was further characterized by UV-vis, fluorescence spectra, and time-resolved fluorescence decay in solution (Figure 2a). The absorption spectrum of **PS1** shows an absorption maximum at 331 nm and an optical bandgap of 3.75 eV, which is slightly blue-shifted compared with those of monomer **8** (maximized at 337 nm) and [8]cyclo-*para*-phenylene (maximized at 340 nm). The absorption coefficient (ϵ) of **8** is $\sim 4.95 \times 10^4 \text{ L cm}^{-1} \text{ mol}^{-1}$. Also, the absorption spectra of polymer **PS1** and **8** display an interesting shoulder peak at ~ 340 nm due to the presence of linear benzene rings.

The fluorescence spectra of **PS1** and **8** show nearly the same maximum peak at ~ 540 nm (Figure 2b). By using anthracene as the reference ($\Phi_F = 30\%$ in ethanol), the fluorescence quantum yield for the **8** and **PS1** were determined to be $\Phi_F = 22\%$ and $\Phi_F = 42\%$, respectively, which are much higher than in [8]cyclo-*para*-phenylene ($\Phi_F = 10\%$).³⁹ The enhanced fluorescence quantum yield of **PS1** may indicate a much longer and more rigid structure. The fluorescence colors of **PS1**, **8**, and [8]cyclo-*para*-phenylene are shown in Figure 2b (inset). Time-resolved fluorescence decay measurements were conducted using a nanosecond pulsed laser system in a degassed CH_2Cl_2 solution at room temperature (Figures

2c-2d). The fluorescence decay of **8** follows first-order kinetics with a lifetime (τ_s) = 7.1 ns at 534 nm when excited at ~ 390 nm. **PS1** shows a similar single-exponential decay with a slightly longer fluorescence lifetime $\tau_s = 7.4$ ns at 534 nm. The similarity of the absorption, fluorescence spectra, and time-resolved fluorescence decay of **PS1** and **8** in solution indicates that these optical properties are primarily governed by the cyclo-*para*-phenylenes and are slightly affected by the linear PPP backbone.

Considering the remarkable electronic properties of carbon nanotubes and related structures⁴⁰⁻⁴² and the novel polymeric structure of **PS1** as a long polymeric segment of carbon nanotubes, we examined the potential application of **PS1** as an electron-transport layer for optoelectronic devices on the electron mobility (μ_e), which is measured by the space charge limited current (SCLC) method.⁴³⁻⁴⁴ Electron-only ITO/ZnO/**PS1**/Ca/Al device was fabricated, as shown in Figure 3 (inset). Then, the μ_e value was calculated using Mott-Gurney equation, revealing that the electron mobility of **PS1** is $\sim 2.0 \times 10^{-5} \text{ cm}^2 \text{ V}^{-1} \text{ s}^{-1}$ in the SCLC region (Figure 3). The measured electron mobility value of the electron-only ITO/ZnO/**PS1**/Ca/Al device indicates that polymer **PS1** is promising for application in the electron-transport layer.

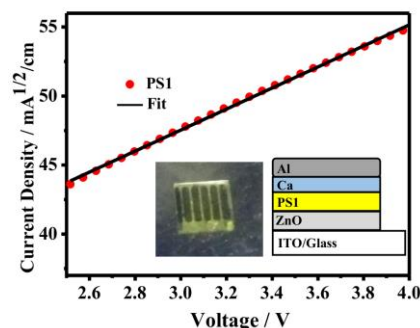


Figure 3. $J^{1/2}$ - V and the corresponding fitting curves of the electron-only ITO/ZnO/**PS1**/Ca/Al devices.

In summary, we successfully synthesized a novel π -extended polymer (**PS1**) containing a cyclo-*para*-phenylene unit and a PPP backbone. **PS1** is constructed entirely from sp^2 -hybridized carbon atoms and represents the first polymeric segment of the armchair [8,8]SWCNT. In the **PS1**, a cyclo-*para*-phenylene unit forms the curved cyclic polyphenylene part in the target CNT and a linear PPP backbone mimics the linear polyphenylene part along the 1D direction of the CNT. With its unique structural and physical properties, this long π -extended polymer **PS1** represents a key step toward the bottom-up synthesis of uniform carbon nanotubes and provides potential applications in electron-transport devices.

ASSOCIATED CONTENT

Supporting Information

Additional experimental data include Synthesis details, ^1H NMR, ^{13}C NMR, HR-MS, 2D NMR. This material is available free of charge via the Internet.

AUTHOR INFORMATION

Corresponding Author

Email: dupignwu@ustc.edu.cn

Notes

The authors declare no competing financial interests.

ACKNOWLEDGMENT

This work was financially supported by the National Key Research and Development Program of China (2017YFA0402800), the National Natural Science Foundation of China (21971229, 51772285), and the Fundamental Research Funds for the Central Universities.

REFERENCES

- Gin, D. L.; Conticello, V. P.; Grubbs, R. H. Stereoregular Precursors to Poly(p-phenylene) via Transition-Metal-Catalyzed Polymerization. 1. Precursor Design and Synthesis. *J. Am. Chem. Soc.* **1994**, *116*, 10507-10519.
- Kovacic, P.; Jones, M. B. Dehydro Coupling of Aromatic Nuclei by Catalyst-Oxidant Systems: Poly(p-phenylene). *Chem. Rev.* **1987**, *87*, 357-379.
- Rehahn, M.; Schlüter, A.-D.; Wegner, G.; Feast, W. J. Soluble poly(*para*-phenylene)s. 1. Extension of the Yamamoto synthesis to dibromobenzenes substituted with flexible side chains. *Polymer* **1989**, *30*, 1054-1059.
- Grem, G.; Martin, V.; Meghdadi, F.; Paar, C.; Stampfl, J.; Sturm, J.; Tasch, S.; Leising, G. Stable poly(*para*-phenylene)s and their application in organic light emitting devices. *Synthetic Met.* **1995**, *71*, 2193-2194.
- Leising, G.; Scherf, U. Electroluminescence devices with poly(paraphenylene) and derivatives as the active material. *Proceedings of SPIE* **1993**, *1910*, 70-77.
- Grem, G.; Leditzky, G.; Ullrich, B.; Leising, G. Realization of a blue-light-emitting device using poly(p-phenylene). *Adv. Mater.* **1992**, *4*, 36-37.
- Strunk, K.-P.; Abdulkarim, A.; Beck, S.; Marszalek, T.; Bernhardt, J.; Koser, S.; Pisula, W.; Jänsch, D.; Freudenberg, J.; Pucci, A.; Bunz, U. H. F.; Melzer, C.; Müllen, K. Pristine Poly(*para*-phenylene): Relating Semiconducting Behavior to Kinetics of Precursor Conversion. *ACS Appl. Mater. Interfaces* **2019**, *11*, 19481-19488.
- Soaresz, J. C.; Foschini, M.; Eiras, C.; Sanches, E. A.; Gonçalves, D. Electrosynthesis and Optical Characterization of Poly(p-phenylene), Polypyrrole and Poly(p-phenylene)-polypyrrole Films. *Mater. Res.* **2014**, *17*, 332-337.
- Ivory, D. M.; Miller, G. G.; Sowa, J. M.; Shacklette, L. W.; Chance, R. R.; Baughman, R. H. Highly Conducting Charge-transfer Complexes of Poly(p-phenylene). *J. Chem. Phys.* **1979**, *71*, 1506-1507.
- Basagni, A.; Sedona, F.; Pignedoli, C. A.; Cattelan, M.; Nicolas, L.; Casarin, M.; Sambri, M. Molecules-Oligomers-Nanowires-Graphene Nanoribbons: A Bottom-Up Stepwise On-Surface Covalent Synthesis Preserving Long-Range Order. *J. Am. Chem. Soc.* **2015**, *137*, 1802-1808.
- Dresselhaus, M. S.; Dresselhaus, G.; Charlier, J. C.; Hernández, E. Electronic, thermal and mechanical properties of carbon nanotubes. *Philos. Trans. R. Soc. London, Ser. A* **2004**, *362*, 2065-2098.
- Terrones, M. Carbon nanotubes: Synthesis and Properties, Electronic Devices and Other Emerging Applications. *Int. Mater. Rev.* **2013**, *49*, 325-377.
- Schroeder, V.; Savagatrup, S.; He, M.; Lin, S.; Swager, T. M. Carbon Nanotube Chemical Sensors. *Chem. Rev.* **2019**, *119*, 599-663.
- Rao, R. P.; Islam, A. E.; Weatherup, R. S.; Hofmann, S.; Meshot, E. R.; Wu, F.; Zhou, C.; Dee, N.; Amama, P. B.; Carpena-Nunez, J.; Shi, W.; Plata, D. L.; Penev, E. S.; Yakobson, B. I.; Balbuena, P. B.; Bichara, C.; Futaba, D. N.; Noda, S.; Shin, H. et al. Carbon Nanotubes and Related Nanomaterials: Critical Advances and Challenges for Synthesis Toward Mainstream Commercial Applications. *ACS Nano* **2018**, *12*, 11756-11784.
- Yang, F.; Wang, X.; Zhang, D.; Yang, J.; Luo, D.; Xu, Z.; Wei, J.; Wang, J.-Q.; Xu, Z.; Peng, F.; Li, X.; Li, R.; Li, Y.; Li, M.; Bai, X.; Ding, F.; Li, Y. Chirality-specific growth of single-walled carbon nanotubes on solid alloy catalysts. *Nature* **2016**, *510*, 522-524.
- Jasti, R.; Bhattacharjee, J.; Neaton, J. B.; Bertozzi, C. R. Synthesis, Characterization, and Theory of [9]-, [12]-, and [18]Cycloparaphenylene: Carbon Nanohoop Structures. *J. Am. Chem. Soc.* **2008**, *130*, 17646-17647.
- Scott, L. T.; Jackson, E. A.; Zhang, Q.; Steinberg, B. D.; Bancu, M.; Li, B. A Short, Rigid, Structurally Pure Carbon Nanotube by Stepwise Chemical Synthesis. *J. Am. Chem. Soc.* **2011**, *134*, 107-110.
- Takaba, H.; Omachi, H.; Yamamoto, Y.; Bouffard, J.; Itami, K. Selective Synthesis of [12]Cycloparaphenylene. *Angew. Chem., Int. Ed.* **2009**, *48*, 6112-6116.
- Bodwell, G. J. Carbon Nanotubes: Growth Potential. *Nat. Nanotechnol.* **2010**, *5*, 103-104.
- Yamago, S.; Watanabe, Y.; Iwamoto, T. Synthesis of [8]Cycloparaphenylene from a Square-Shaped Tetranuclear Platinum Complex. *Angew. Chem., Int. Ed.* **2010**, *49*, 757-759.
- Gölling, F. E.; Quernheim, M.; Wagner, M.; Nishiuchi, T.; Müllen, K. Concise Synthesis of 3D π -Extended Polyphenylene Cylinders. *Angew. Chem., Int. Ed.* **2014**, *53*, 1525-1528.
- Guo, L. F.; Yang, X. D.; Cong, H. Synthesis of Macrocyclic Oligoparaphenylenes Derived from Anthracene Photodimer. *Chin. J. Chem.* **2018**, *36*, 1135-1138.
- Li, H. B.; Page, A. J.; Irle, S.; Morokuma, K. Theoretical Insights into Chirality-Controlled SWCNT Growth from a Cycloparaphenylene Template. *ChemPhysChem* **2012**, *13*, 1479-1485.
- Wassy, D.; Pfeifer, M.; Esser, B. Synthesis and Properties of Conjugated Nanohoops Incorporating Dibenzo[a, e]pentalenes: [2]DBP[12]CPPs. *J. Org. Chem.* **2019**, 10.1021/acs.joc.1029b01195. published online.
- Cheung, K. Y.; Gui, S. J.; Deng, C. F.; Liang, H. F.; Xia, Z. M.; Liu, Z.; Chi, L. F.; Miao, Q. Synthesis of Armchair and Chiral Carbon Nanobelts. *Chem* **2019**, *5*, 838-847.
- Lu, D.; Zhuang, G.; Wu, H.; Wang, S.; Yang, S.; Du, P. A Large π -Extended Carbon Nanoring Based on Nanographene Units: Bottom-Up Synthesis, Photophysical Properties, and Selective Complexation with Fullerene C₇₀. *Angew. Chem., Int. Ed.* **2017**, *56*, 158-162.
- Povie, G.; Segawa, Y.; Nishihara, T.; Miyauchi, Y.; Itami, K. Synthesis of a carbon nanobelt. *Science* **2017**, *356*, 172-175.
- Huang, Q.; Zhuang, G. L.; Jia, H. X.; Qian, M. M.; Cui, S. S.; Yang, S. F.; Du, P. W. Photoconductive Curved-Nanographene/Fullerene Supramolecular Heterojunctions. *Angew. Chem., Int. Ed.* **2019**, *58*, 6244-6249.
- Huang, C.; Huang, Y.; Akhmedov, N. G.; Popp, B. V.; Petersen, J. L.; Wang, K. K. Functionalized Carbon Nanohoops: Synthesis and Structure of a [9]Cycloparaphenylene Bearing Three 5,8-Dimethoxynaphthyl-1,4-diyl Units. *Org. Lett.* **2014**, *16*, 2672-2675.
- Farajidizaji, B.; Huang, C.; Thakellapalli, H.; Li, S.; Akhmedov, N. G.; Popp, B. V.; Petersen, J. L.; Wang, K. K. Synthesis and Characterization of Functionalized [12]Cycloparaphenylenes Containing Four Alternating Biphenyl and Naphthyl Units. *J. Org. Chem.* **2017**, *82*, 4458-4464.
- Huang, Z.-A.; Chen, C.; Yang, X.-D.; Fan, X.-B.; Zhou, W.; Tung, C.-H.; Wu, L.-Z.; Cong, H. Synthesis of Oligoparaphenylene-Derived Nanohoops Employing an Anthracene Photodimerization-Cycloreversion Strategy. *J. Am. Chem. Soc.* **2016**, *138*, 11144-11147.
- Xu, Y. Z.; Wang, B. Z.; Kaur, R.; Minameyer, M. B.; Bothe, M.; Drewello, T.; Guldi, D. M.; von Delius, M. A supramolecular [10]CPP junction enables efficient electron

- transfer in modular porphyrin-[10]CPP superset of fullerene complexes. *Angew. Chem., Int. Ed.* **2018**, *57*, 11549-11553.
- (33) Hitosugi, S.; Nakanishi, W.; Yamasaki, T.; Isobe, H. Bottom-Up Synthesis of Finite Models of Helical (n,m)-Single-Wall Carbon Nanotubes. *Nat. Commun.* **2011**, *2*, 492.
- (34) Fort, E. H.; Donovan, P. M.; Scott, L. T. Diels-Alder Reactivity of Polycyclic Aromatic Hydrocarbon Bay Regions: Implications for Metal-Free Growth of Single-Chirality Carbon Nanotubes. *J. Am. Chem. Soc.* **2009**, *131*, 16006-16008.
- (35) Sanchez-Valencia, J. R.; Dienel, T.; Groning, O.; Shorubalko, I.; Mueller, A.; Jansen, M.; Amsharov, K.; Ruffieux, P.; Fasel, R. Controlled synthesis of single-chirality carbon nanotubes. *Nature* **2014**, *512*, 61-65.
- (36) Liu, B.; Liu, J.; Li, H.-B.; Bhola, R.; Jackson, E. A.; Scott, L. T.; Page, A.; Irle, S.; Morokuma, K.; Zhou, C. Nearly Exclusive Growth of Small Diameter Semiconducting Single-Wall Carbon Nanotubes from Organic Chemistry Synthetic End-Cap Molecules. *Nano Lett.* **2015**, 586-595.
- (37) Abdulkarim, A.; Hinkel, F.; Jansch, D.; Freudenberg, J.; Golling, F. E.; Müllen, K. A New Solution to an Old Problem: Synthesis of Unsubstituted Poly(para-phenylene). *J. Am. Chem. Soc.* **2016**, *138*, 16208-16211.
- (38) Chen, H.; Golder, M. R.; Wang, F.; Jasti, R.; Swan, A. K. Raman spectroscopy of carbon nanohoops. *Carbon* **2014**, *67*, 203-213.
- (39) Darzi, E. R.; Sisto, T. J.; Jasti, R. Selective Syntheses of [7]-[12]Cycloparaphenylenes Using Orthogonal Suzuki-Miyaura Cross-Coupling Reactions. *J. Org. Chem.* **2012**, *77*, 6624-6628.
- (40) Fischer, J. E.; Johnson, A. T. Electronic properties of carbon nanotubes. *Curr. Opin. Solid State Mater. Sci.* **1999**, *4*, 28-33.
- (41) Tameev, A. R.; Pereshivko, L. Y.; Vannikov, A. V. Charge Carrier Mobility in Films of Carbon-Nanotube-Polymer Composites. *Mol. Cryst. Liq. Cryst.* **2008**, *497*, 333-338.
- (42) Kayahara, E.; Sun, L.; Onishi, H.; Suzuki, K.; Fukushima, T.; Sawada, A.; Kaji, H.; Yamago, S. Gram-Scale Syntheses and Conductivities of [10]Cycloparaphenylene and Its Tetraalkoxy Derivatives. *J. Am. Chem. Soc.* **2017**, *139*, 18480-18483.
- (43) Blom, P. W. M.; de Jong, M. J. M.; Vleggaar, J. J. M. Electron and hole transport in poly(p-phenylene vinylene) devices. *Appl. Phys. Lett.* **1996**, *68*, 3308-3310.
- (44) Mihailetschi, V. D.; Wildeman, J.; Blom, P. W. M. Space-Charge Limited Photocurrent. *Phys. Rev. Lett.* **2005**, *94*, 126602.

Insert Table of Contents artwork here

